Some Implications of Core Regime Wind Structures in Western North Pacific Tropical Cyclones

DELIA YEN-CHU CHEN

Department of Atmospheric Sciences, National Taiwan University, Taipei, Taiwan

KEVIN K. W. CHEUNG

Department of Environment and Geography, and Climate Futures Research Centre, Macquarie University, Sydney, New South Wales, Australia

CHENG-SHANG LEE

Department of Atmospheric Sciences, National Taiwan University, and Taiwan Typhoon and Flood Research Institute, National Applied Research Laboratories, Taipei, Taiwan

(Manuscript received 12 March 2010, in final form 29 July 2010)

ABSTRACT

In this study, a tropical cyclone (TC) is considered to be compact if 1) the radius of maximum wind or the maximum tangential wind is smaller than what would be expected for an average tropical cyclone of the same intensity or the same radius of maximum wind, and 2) the decrease of tangential wind outside the radius of maximum wind is greater than that of an average TC. A structure parameter *S* is defined to provide a quantitative measure of the compactness of tropical cyclones. Quick Scatterometer (QuikSCAT) oceanic winds are used to calculate *S* for 171 tropical cyclones during 2000–07. The *S* parameters are then used to classify all of the cases as either compact or incompact according to the 33% and 67% percentiles. It is found that the early intensification stage is favorable for the occurrence of compact tropical cyclones, which also have a higher percentage of rapid intensification than incompact cases. Composite infrared brightness temperature shows that compact tropical cyclones have highly axisymmetric convective structures with strong convection concentrated in a small region near the center. Low-level synoptic patterns are important environmental factors that determine the degree of compactness; however, it is believed that compact tropical cyclones maintain their structures mainly through internal dynamics.

1. Introduction

To improve forecasts of tropical cyclone (TC) impacts, better predictions of TC intensity and structure are required. In response to these demands, extensive research on TC intensification and structure change has been carried out, and forecast products such as intensity forecasts and quantitative precipitation forecasts that are available for applications in operational centers have also increased. For example, recent studies have analyzed several physical mechanisms that impact TC intensification, including maximum potential intensity (MPI) theory (Emanuel 1988; DeMaria and Kaplan 1994b; Holland 1997), vertical wind shear (Frank and Ritchie 2001; Emanuel et al. 2004; Knaff et al. 2004), the terrain effect (Cubukcu et al. 2000), internal dynamic processes (Black and Willoughby 1992; Guinn and Schubert 1993; Schubert et al. 1999; Kossin and Eastin 2001; Kuo et al. 2009), and ocean heat content (Schade 2000; Emanuel et al. 2004; Lin et al. 2008; Mainelli et al. 2008). These factors that can influence changes in typhoon intensity have also been examined using numerical experiments (e.g., DeMaria 1996; Bender and Ginis 2000; Frank and Ritchie 2001). Furthermore, using advances in observation techniques over the oceans and progress in developing an air–sea coupled model, Lin et al. (2005) and Wu et al. (2007) showed that warm ocean eddies play an important role in typhoon intensity changes.

Corresponding author address: Cheng-Shang Lee, Department of Atmospheric Sciences, National Taiwan University, Taipei 10617, Taiwan.
E-mail: cslee@ntu.edu.tw

DOI: 10.1175/2010WAF2222420.1

The problems related to typhoon size and size change have been discussed over the past few decades (e.g., Brand 1972; Frank and Gray 1980; Merrill 1984; Liu and Chan 1999; Cocks and Gray 2002). In a recent study of typhoon size, Lee et al. (2010) applied Quick Scatterometer (QuikSCAT) oceanic winds data to analyze changes in TC size, which is defined as the radius of 15 m s^{-1} tangential wind, in the western North Pacific (WNP) from 2000 to 2005. Results from Lee et al. show that if a TC is relatively large (small) when developing to tropical storm intensity, it has a 70% (65%) probability of remaining in the same size category upon reaching typhoon intensity. In other words, there is a tendency for a TC to retain its size category during the intensification phase from tropical storm to typhoon.

Holland and Merrill (1984) defined typhoon structure using three properties: intensity, strength, and size. Unlike intensity and size, there have been relatively fewer studies regarding typhoon strength. Weatherford and Gray (1988) showed that outer-core strength (OCS; defined as the mean tangential wind speed for radii at 1°–2.5°) has a strong positive relationship with size (defined as the radius of 15 m s^{-1} wind). In addition, inner-core strength (ICS; defined as the mean tangential wind speed between 65 and 140 km from the storm center) has been shown to be linearly correlated with intensity (Croxford and Barnes 2002). Such results show that using different azimuthal bands to calculate strength might reveal different storm structures. Therefore, analyses that investigate variations of the wind field within a radius of about 300 km and that identify the physical mechanisms responsible for these variations are important for improving both the theoretical understanding of TC structure and operational forecasts. For example, using aircraft reconnaissance flight-level data, Maclay et al. (2008) calculated the low-level area-integrated kinetic energy (KE) within 200 km of some Atlantic and eastern Pacific TCs. Through analyses of KE, Maclay et al. showed different structure evolution patterns and responsible mechanisms. In the latter consideration, note that variation in the inner-core wind field affected the area that contained destructive winds and the radial extent of the strong vorticity region.

This study focuses on the structure of the so-called compact typhoons with strong, highly axisymmetric winds concentrated mostly near the radius of maximum wind (RMW). These compact typhoons generally are intense and possess relatively small RMWs. Knaff et al. (2003, 2008) analyzed another group of TCs, termed annular hurricanes (AHs), which share some common features with compact typhoons, such as few or no rainband structures. In contrast to compact typhoons, AHs have eye sizes larger than the average value with symmetrically distributed eyewall convection, which implies that they have fairly large radii of maximum wind. Statistically, AHs tend to maintain their peak intensity longer and weaken more slowly than the average hurricane.

The following examples clearly show the impact of TC structure on damage potential. Typhoon Toraji (2001), which is identified as a compact typhoon based on the methodology in this study, made landfall in Taiwan with an estimated maximum sustained wind of 38 m s^{-1} (10-min average; observed by the Central Weather Bureau of Taiwan) and a minimum mean sea level pressure of 962 hPa. Radar reflectivity images show that Typhoon Toraji possessed an extremely compact structure with deep convection areas concentrated within only 25 km from the center (Fig. 1a). As a consequence, the 3-h accumulated rainfall of 390 mm recorded at 1800 UTC 29 July was near the landfall position where severe debris flow and other damage occurred, but the rain rate farther away was much less. A few years later, Typhoon Kaemi (2006) impacted Taiwan with an intensity that was comparable to that of Typhoon Toraji at landfall (38 m s^{-1}, 960 hPa, observed by Central Weather Bureau of Taiwan). Typhoon Kaemi was an incompact case, which is revealed by its more extensive and asymmetric convective structure (Fig. 1b). The maximum 3-h accumulated rainfall associated with Typhoon Kaemi as recorded by stations near the track after landfall was only about 100 mm. Comparatively, the hazards brought by Typhoon Kaemi were much less than those from Toraji. While these two examples do not necessarily represent typical rainfall scenarios given their sizes, they show that a typhoon with a compact structure can still cause enormous damage.

Forecasters are likely to underestimate the impacts from compact typhoons because of the relatively small radius of the major convection area. The size of a compact typhoon makes forecasts even more challenging because the degree of damage can vary greatly within a short distance from the landfall region to areas just tens of kilometers away. However, it is difficult to explore issues related to the development of compact typhoons because of the lack of ground truth observations over the vast ocean. Furthermore, the methodologies in studies such as Powell and Reinhold (2007) and Maclay et al. (2008) were not designed to represent compact TCs. Accordingly, this study attempts to identify the general characteristics of compact typhoons as revealed by satellite observations.

To begin the examination of such special typhoon structures, section 2 describes the various datasets used in this study. The methodology used to calculate the structure parameters is presented in section 3. Section 4 contains several case studies of compact and incompact

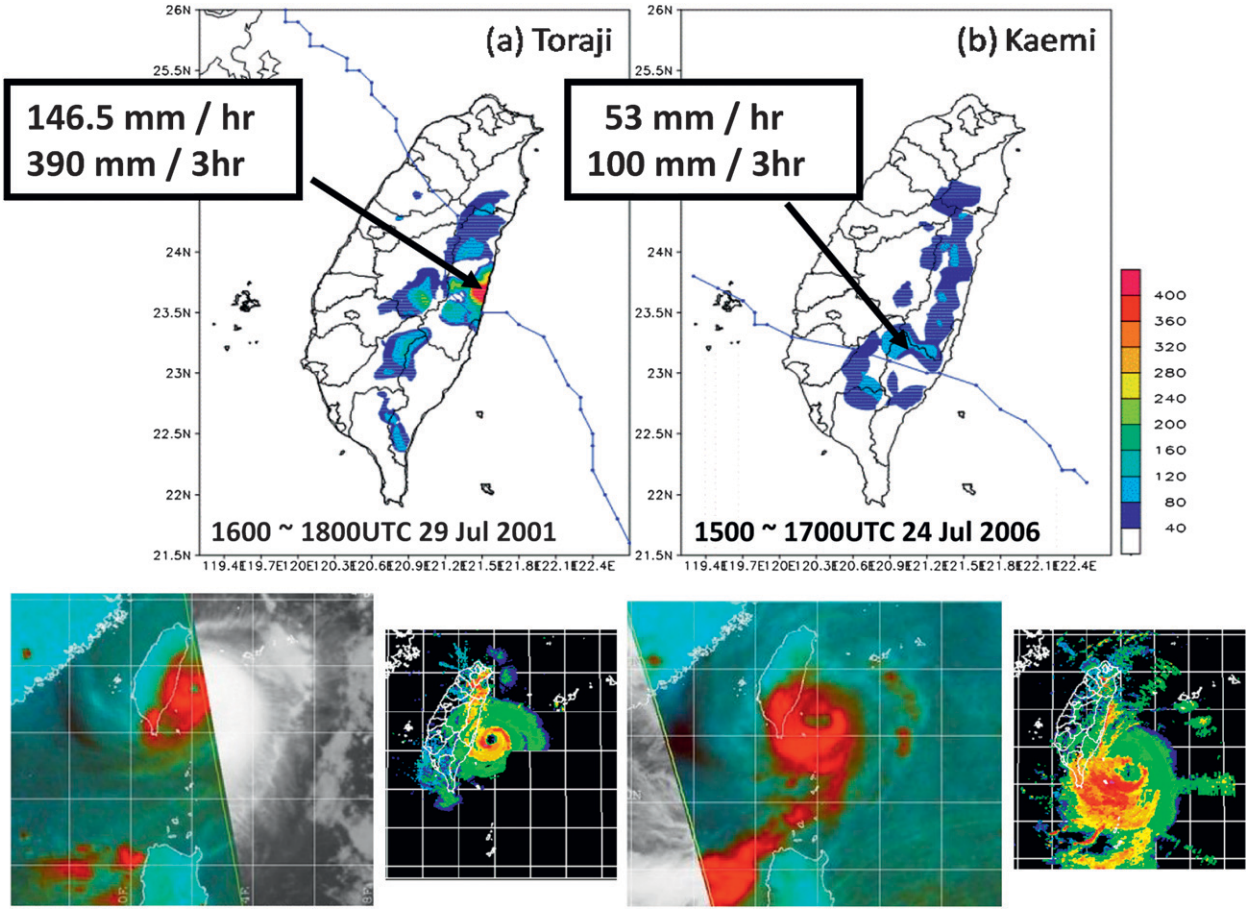

FIG. 1. (a) Observed accumulated station rainfall during 1600–1800 UTC 29 Jul 2001 (shaded) and best track (blue line) for Typhoon Toraji; (bottom left) enhanced infrared satellite imagery from *GMS-5* and radar reflectivity from the Central Weather Bureau of Taiwan. (b) As in (a), except during the period of 1500–1700 UTC 24 Jul 2006 for Typhoon Kaemi, with satellite imagery from MTSAT-1R.

typhoons, as well as their climatological characteristics. Section 5 provides a summary and discussion.

2. Data treatment

The position and intensity of each tropical cyclone at 6-h intervals is obtained from the best-track dataset of the Joint Typhoon Warning Center (JTWC). The reported intensity data in the JTWC best tracks represent 1-min average maximum wind at 10-m altitude (Guard et al. 1992). After 2004, the JTWC best-track dataset also includes the RMW and the radii of 34-, 50-, 64-, and 100-kt winds (1 kt = 0.514 m s^{-1}) in the four quadrants. A cubic spline interpolation scheme is used to interpolate the 6-hourly best-track data to obtain hourly positions.

To investigate the surface wind distribution of TCs, QuikSCAT oceanic 10-m winds, which are derived from microwave scatterometer data, are used (Boukabara et al. 2002; Weissman et al. 2002). The QuikSCAT wind data correspond to surface winds with a time averaging period of 8–10 min. The QuikSCAT data are available twice a day starting from June 1999 on a 25-km grid. The QuikSCAT winds generally agree well with those taken by ocean buoys (Ebuchi et al. 2002; Pickett et al. 2003; Sharma and D'Sa 2008). To have more than 50% data coverage for each of the TCs, only those QuikSCAT swath data that include the tropical cyclone center are used in the analysis. In addition, the scatterometer data that are contaminated by rain (i.e., with rain flag signals) are removed because these data are less accurate (Weissman et al. 2002). With the above mentioned criteria, a total of 1252 time periods for 171 TCs during 2000–07 are available for analyses.

QuikSCAT wind speed varies substantially along the azimuth (Bourassa et al. 2003; Brennan et al. 2009). Therefore, a special consideration is adopted to determine the maximum tangential wind and the RMW. The maximum tangential wind speed (Vt_{max}) is taken to be the average of the top 1% of all tangential wind speeds within 250 km from the TC center. The RMW is

then determined from the average of the radii corresponding to those high wind speeds. Similarly, the tangential wind speed at two times the RMW (Vt_{2RMW}) is also taken to be the average of the 1% wind speeds located closest to the radius of 2RMW.

Infrared satellite images from a digital archive at Kochi University in Japan are used to examine convection. The hourly infrared channel-1 (IR1) cloud-top temperature dataset is on a 5-km grid with a spatial coverage of 20°S–70°N, 70°–160°E. This IR1 dataset includes three different satellite platforms: *Geostationary Meteorological Satellite-5* (*GMS-5*; June 1995–May 2003), *Geostationary Operational Environmental Satellite-9* (*GOES-9*; May 2003–July 2005), and the *Multifunctional Transport Satellite-1R* (*MTSAT-1R*; July 2005–present). In addition, examination of the synoptic environment associated with the TCs is based on analyses of the Global Forecast System (GFS) of the National Centers for Environmental Prediction (NCEP) on a 1° × 1° latitude–longitude grid.

3. TC structural analysis

a. Parameters representing the compactness of a TC

Although parameters such as intensity, strength, and size can be used to describe the structure of a TC individually, none of them provides adequate information regarding the compactness of wind structure at inner radii. Therefore, a new parameter is defined in this study to examine the compactness of a TC.

Weatherford and Gray (1988) showed that more intense TCs tend to possess smaller eyewall radii or RMWs. A compact TC is considered to have a smaller RMW for a given intensity compared with other TC cases. To quantitatively measure the decreasing rate of wind speed with increasing radius, wind speed at 2RMW is examined. Linear regression between the maximum tangential wind (Vt_{max}) and the tangential wind speed at 2RMW (Vt_{2RMW}) suggests that the value of Vt_{2RMW} is roughly half of that of Vt_{max} (statistically the ratio of Vt_{2RMW} to Vt_{max} has an average of 0.49 and a standard deviation of 0.13). Such a relationship can be explained by the conservation of angular momentum. Following Holland (1983), the absolute angular momentum (M_a) is defined as

$$M_a = M_r + M_e = rV_\theta + \frac{1}{2} f_0 r^2, \tag{1}$$

where M_r is the relative angular momentum (RAM), M_e the earth angular momentum (EAM), V_θ the tangential wind at radius r, and f_0 the Coriolis parameter at the center. If the meridional motion of a TC is assumed to be small, a change in f_0 over a short time interval is small and thus the change of the EAM term in the angular momentum equation can be neglected. Consequently, an air parcel would increase its tangential wind speed as it moves toward the center because of the conservation of angular momentum. Examination of the radial profiles of tangential winds (Vt) for all TCs in this study reveals that in the compact cases Vt decrease substantially from RMW to 2RMW. Therefore, a TC is considered compact if 1) its RMW or Vt_{max} is smaller than what would be expected for an averaged TC with the same intensity or the same RMW, and 2) the decrease of Vt from RMW to 2RMW is greater than that of an average TC.

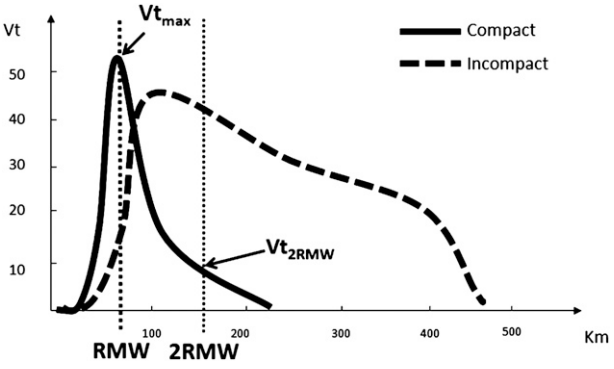

FIG. 2. Schematic showing the definition of Vt_{max}, Vt_{2RMW}, RMW, and 2RMW. Typical structures of a compact TC (solid line) and an incompact TC (dashed line) are shown.

To quantitatively describe the structural characteristics in accordance with the above two conditions, a dimensionless structure parameter S is defined as follows:

$$S = \frac{Vt_{2RMW}}{Vt_{max}} \times \frac{(RMW \times Vt_{max})}{(Vt_{2RMW} \times RMW)_{ave}} = \frac{Vt_{2RMW} \times RMW}{(Vt_{2RMW} \times RMW)_{ave}}, \tag{2}$$

where $(Vt_{2RMW} \times RMW)_{ave}$ is the average value of the product of Vt_{2RMW} and RMW for all TC cases analyzed in this study. The purpose of using $(Vt_{2RMW} \times RMW)_{ave}$ instead of $(Vt_{max} \times RMW)_{ave}$ in (2) is to normalize the values of S (note that the average value of S for all TCs in this study is 1). The other terms are as defined before (Fig. 2). The S parameter is expected to be relatively small ($S < 1$) for a compact TC because the ratio of Vt_{2RMW} to Vt_{max} is small (criterion 2), and the RMW is smaller than an average TC with that same intensity (criterion 1). However, note that including only the value of RMW (or its ratio to the average value) in the definition of S is inadequate because climatologically RMW does decrease during intensification. Examination of the product of RMW and intensity allows for the

TABLE 1. The *S* parameter values that measure compactness for different Vt_{max}, RMW, and *b* in the CW vortex. The boldface values indicate the smallest *S* in each group.

Exp	Vt_{max}	RMW	*b*	*S*
B1	40	80	0.8	1.73
B2	40	80	1.0	1.63
B3	40	80	1.2	**1.52**
R1	40	60	1.0	**1.22**
R2	40	80	1.0	1.63
R3	40	100	1.0	2.03
V1	30	80	1.0	**1.22**
V2	40	80	1.0	1.63
V3	50	80	1.0	2.03
S1	35	80	0.97	**1.44**
S2	40	80	1.29	1.47
S3	50	80	1.74	1.51

identification of compact TCs with exceptionally small RMW values when the intensity is taken into account (i.e., TC cases that intensify to similar intensities are compared).

b. The S parameter for idealized vortices

To illustrate how the parameter *S* changes for TCs with different structures, various idealized vortices are analyzed. For this purpose, the modified Rankine vortex structures as that applied in Chan and Williams (1987) for studying the beta propagation effect on TC motion (the ''CW vortex'') are examined. The tangential wind structure in the CW vortex is given by

$$\mathrm{Vt}(r) = \mathrm{Vt}_{\max}\left(\frac{r}{\mathrm{RMW}}\right)\exp\left\{\frac{1}{b}\left[1-\left(\frac{r}{\mathrm{RMW}}\right)^{b}\right]\right\}, \quad (3)$$

and the relative vorticity can be written as follows:

$$\xi(r) = \frac{2\mathrm{Vt}_{\max}}{\mathrm{RMW}}\left[1-\frac{1}{2}\left(\frac{r}{\mathrm{RMW}}\right)^{b}\right]\exp\left\{\frac{1}{b}\left[1-\left(\frac{r}{\mathrm{RMW}}\right)^{b}\right]\right\}. \quad (4)$$

There are three parameters in the above equation, namely, Vt_{max}, RMW, and *b*, which determine the structure of a CW vortex. In particular, the parameter *b* determines the rate of decrease of the tangential wind speed with a given radius (*b* is usually positive and a larger value of *b* yields a faster decreasing rate of the tangential wind speed outside the RMW).

Sensitivity of the *S* parameter to three parameters controlling the CW vortex structure is explored through several sets of calculations, in each of which only one parameter is changed (Table 1). In the first set (B1–B3), only the *b* parameter is allowed to vary; results show that a large *b* value leads to a small *S* parameter because the ratio of Vt_{2RMW} to Vt_{max} is small with a faster rate of decrease in the tangential wind speed. In the second set (R1–R3), a smaller RMW yields a smaller *S* value given fixed intensity and *b* in accord with the definition of *S*. The calculations V1–V3 in the third set have fixed RMW and *b* values, but the intensity is allowed to vary. This is one of the intensification models considered by Carr and Elsberry (1997) in which wind speeds at the RMW and outer radii increase by a similar amount (such that the radial profile of wind speed stays fairly constant during intensification). Under such conditions (both RMW and *b* are fixed), a TC is more compact (*S* is smaller) if its intensity is weaker. Another intensification model considered by Carr and Elsberry (1997) is that the increase of the wind speed concentrates near the RMW such that Vt_{2RMW} does not change much; consequently, the decreasing rate of wind speed with radius increases (i.e., larger *b* value). The purpose of doing this experiment is to test criterion 1 by comparing vortices with the same RMW but different Vt_{max} values. The less intense vortex is the slightly more compact one, which means that a much weaker storm can maintain the same RMW as a more intense TC does. These experiments are represented in the set of calculations S1–S3 in Table 1, which indicate that this mode of intensification does lead to a less compact structure [resulting from the increased ($\mathrm{RMW} \times \mathrm{Vt}_{\max}$) factor in the definition of S] but not as much as in the earlier mode. Nevertheless, the RMW is assumed to be constant in the above idealized considerations.

4. Characteristics of compact typhoons

a. Relationships of the S parameter to strength and size

Because the uncertainty of the QuikSCAT winds increases under the high wind speed conditions that usually occur near the typhoon core region, the JTWC best tracks are first used to check the quality of the QuikSCAT data. The factor 0.88 is used to convert the 1-min average wind speed reported in the JTWC best tracks to the 10-min average that is closer to the averaging time period for QuikSCAT winds (Krayer and Marshall 1992; Sampson et al. 1995). The results show that the QuikSCAT-derived intensity has an upper limit of about 50 m s^{-1} and sometimes slightly underestimates (35.3% of all cases, with a threshold of 10 m s^{-1}) or slightly overestimates (31.5% of all cases, with the same threshold) the intensity reported by the JTWC. Overall, only 10% of the data have an error of more than 20 m s^{-1} wind speed difference. Nevertheless, the correlation coefficient between the intensity data from the two sources is 0.73, which indicates that the QuikSCAT-derived data are quite representative of the variability in intensity.

Moreover, the JTWC best-track estimates of the RMW and radii of 34-, 50-, 64-, and 100-kt wind data compared with those inferred from QuikSCAT. Although QuikSCAT winds are likely used in the JTWC estimate of RMW, their operational process also involves subjective determination and in-house climatologies and analysis methods. A detailed examination shows that the QuikSCAT data can generally represent the typhoon wind profile near the inner-core region well. It is initially suspected that the QuikSCAT data underestimate the wind speed in the inner-core region. However, in over 80% of cases the QuikSCAT wind profile agrees with information in the JTWC best-track data (Fig. 3a). In some cases, the QuikSCAT wind speeds are slightly higher than those in the best-track data (Fig. 3b), but in most of these cases the QuikSCAT radial wind profiles suggest similar structures as indicated by the best-track wind radii. Therefore, application of the QuikSCAT winds in computing the TC structure parameters should be justified.

The *S* parameter defined in this study is then compared with the more commonly known concept of strength that measures the TC structure outside the RMW but within the boundary suggested by the TC size. In previous studies, strength values have been calculated for different azimuthal bands (Merrill 1984; Holland and Merrill 1984; Weatherford and Gray 1988; Croxford and Barnes 2002). Here strength is calculated as the average tangential wind speed within the range of 100–300 km from the center. The scatterplot between strength and *S* parameters for all 171 TC cases, which are both inferred from QuikSCAT data, shows a highly linear relationship with a correlation coefficient of 0.83 (Fig. 4a). Therefore, the *S* parameter can also be considered as a certain measure of TC strength and at the same time it provides more information regarding relative wind speeds at the inner core and those outside the core region.

As the modes of intensification discussed in Carr and Elsberry (1997) show, increases in the inner-core wind speeds are not necessarily followed by increases in the regions with larger radii, and thus intensity and strength need not correlate well with each other. This view agrees with previous studies, such as Weatherford and Gray (1988), which indicated that changes in intensity and strength occur quite independently. Although the linear relationship between the *S* parameter and strength is strong (with a correlation coefficient of 0.83; see Fig. 4a), the relationship between the *S* parameter and intensity is only moderate (with a correlation coefficient of 0.54; see Fig. 4b). Next, the discussion turns to the relationship between the *S* parameter and TC size, with the latter being computed based on a radius of 15 m s^{-1} wind speed (R15) using the QuikSCAT winds (Lee et al. 2010). Nevertheless, the *S* parameter describes the radial wind profile from the eyewall up to two times the RMW, and as expected it is closely related to the outer-core wind speeds that determine TC size. Therefore, similar to the high correlation between strength and size found by Weatherford and Gray (1988), a high correlation between the *S* parameter and TC size based on the TC cases in this study is also found (with a correlation coefficient of 0.76, Fig. 4c). At this point, it should be emphasized that the *S* parameter is not supposed to

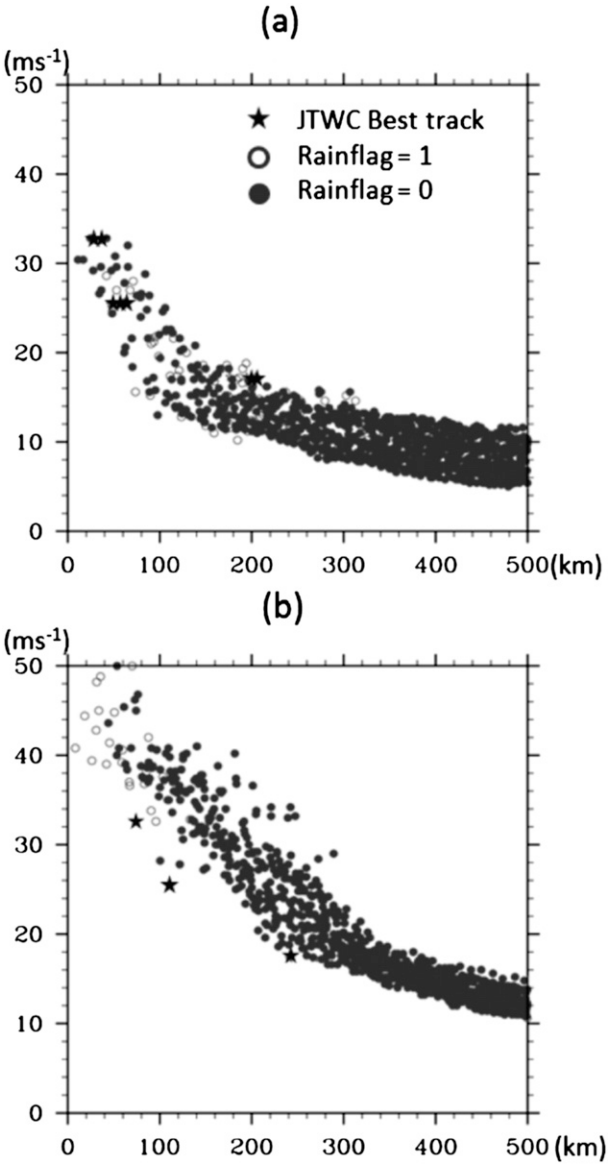

FIG. 3. Wind speed profile at (a) 2014 UTC 27 Sep 2005 for Typhoon Longwang and (b) 2105 UTC 29 Aug 2005 for Typhoon Talim. Best-track data for different quadrants (stars), QuikSCAT data with rain flag signals (open circles), and QuikSCAT data without rain flag signals (closed circles) are shown.

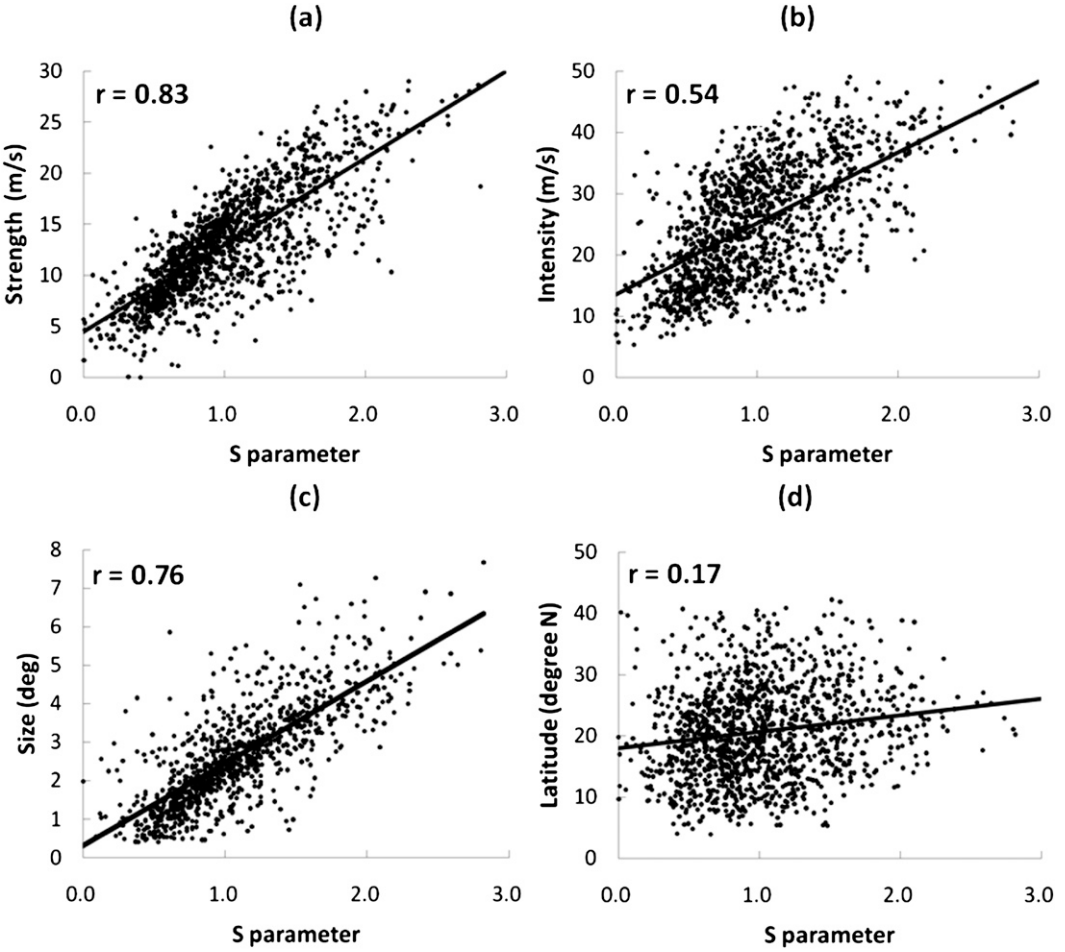

FIG. 4. Scatterplot of S vs (a) strength (m s^{-1}), (b) intensity (m s^{-1}), (c) size (°), and (d) latitude (°N). The best-fit regression lines are indicated (thick lines). The correlation coefficients in all four panels are statistically significant at the 99% confidence level.

replace other measures of strength or size, although it serves to identify the kind of compact typhoon structure that the traditional parameters do not capture thoroughly.

It will be shown in the following analyses that most compact TCs occur at their early development stage and usually at lower latitudes. However, in the WNP there is large variability in the track types at subsequent development stages of TCs when they have changes in size, which is attributed to the relatively lower correlation between the S parameter and latitude (Fig. 4d).

b. Climatological characteristics

Knaff et al. (2003, 2008) revealed that AHs tend to maintain their peak intensity longer and weaken more slowly than average hurricanes, and thus the natural question is whether compact typhoons have similar characteristics, especially when they are compared to incompact typhoons. For this purpose, all TC cases are first categorized as being either compact, moderate, or incompact according to the 33% and 67% percentiles of the S parameter (0.79 and 1.18, respectively). Then, the numbers of compact and incompact typhoons are examined for various intensity categories (Fig. 5). Note that during this classification, the intensifying stage and the weakening stage are distinguished. The distribution of the compact and incompact TCs with respect to different intensity categories shows that during the early development phase (from tropical disturbance to tropical storm) the percentage of compact TCs is noticeably larger than that of incompact TCs. This should be related to the fact that TCs generally grow in size during their life cycle and particularly during weakening (Merrill 1984; Knaff and Zehr 2007; Maclay et al. 2008). For cases with typhoon and supertyphoon intensity and those that have started weakening, the percentage of compact

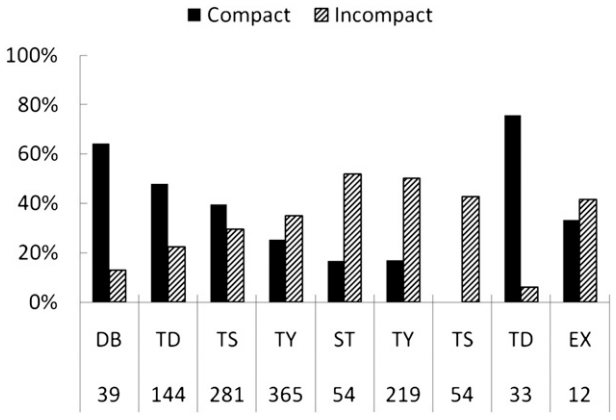

FIG. 5. Histogram of the percentage distribution of TC development stages. Compact cases (black bars) and incompact cases (hatched bars) are represented. The categories of development stages are DB (disturbance), TD (tropical depression), TS (tropical storm), TY (typhoon), ST (supertyphoon), and EX (extratropical system). The numbers represent the case counts for each group.

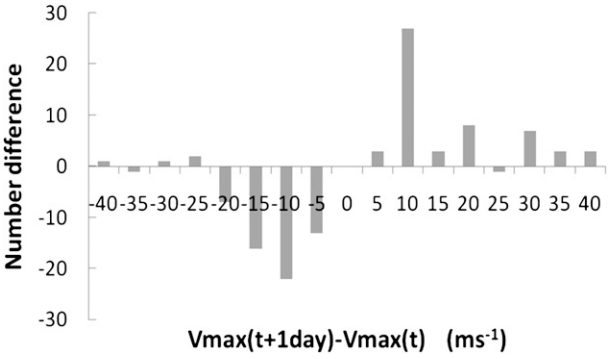

FIG. 6. Histogram of the difference in the number of cases for various 24-h intensity change (m s^{-1}) categories between compact TCs and incompact TCs. A positive number difference means there are more compact TCs.

typhoons is much lower. Therefore, although compact TCs may not reach very strong intensities, they are relatively more conducive to early intensification. After peak intensities are reached, some compact TCs become incompact, which is likely related to factors that lead to weakening, such as movement to higher latitudes (Fig. 4d) and large vertical wind shear. An analysis divide by moving direction (figure not shown) shows that more incompact cases occurred with northward-moving TCs, while mostly compact cases occurred within westward-moving TCs. As a consequence, the number of compact TCs found in the weakening categories in Fig. 5 is much less.

To further explore the relationship between compactness and intensification, the 24-h intensity changes (for minimizing the effect from diurnal variation of convection) for the compact and incompact TCs are calculated and put into binned distributions, respectively. The difference between the distributions of intensity change for these two types of typhoons (Fig. 6) clearly shows that compact TCs are associated with moderate intensification rates (about 10 m s^{-1} increase in wind speed per 24 h). Indeed, more compact TCs undergo rapid intensification (a 30–40 m s^{-1} increase in wind speed per 24 h) than incompact cases. On the other side of the difference distribution (Fig. 6), incompact TCs dominate in the bins with the most common decreasing intensity (5–20 m s^{-1} decrease in wind speed per 24 h). Again, these results suggest that compactness mainly occurs in the development and intensification phases of TCs and is also favorable at lower latitudes.

To focus on wind field and convection characteristics during the development or intensifying stage, all TCs are reclassified as compact, moderate, and incompact cases for their periods with increasing intensities only. The new 33% and 67% percentiles of the S parameter are 0.77 and 1.13, respectively.

Previous studies have shown that infrared (IR) satellite data can be used to estimate vortex structure in TCs (Mueller et al. 2006; Kossin et al. 2007), and thus these kinds of data are applied to compare the compact and incompact TCs. The composite IR1 cloud-top temperatures show that the incompact TCs have a broad region of convection at the TD stage with temperatures lower than 250 K over a domain of about 10° latitude × 20° longitude (Fig. 7a). In contrast, the corresponding convection area of the compact cases has a radius of only about 2° latitude, with a nearly axisymmetric pattern (Fig. 7b). Note that the incompact cases have significant environmental convection surrounding the core region. This major difference in the areal coverage of convection between the compact and the incompact cases persists until the later stages with stronger intensities. For the incompact TCs, convection at about 10° latitude south of the center remains stronger when the TCs intensify to typhoon and supertyphoon (Fig. 7g). On the other hand, the compact TCs have little convection to the south, and they maintain core-region convection throughout the intensification period. For those that intensify to supertyphoons, the cloud-top temperatures in the northeast quadrant appear to be midlatitude systems that interact with the TCs (Fig. 7h). Overall, these composite IR1 imageries suggest strong environmental influences during the intensification of incompact TCs, while internal dynamics may determine the intensification rate of compact TCs.

This assertion is supported by the composite QuikSCAT wind profiles along the east–west direction that crosses the TC center (Fig. 8). The incompact TCs start from

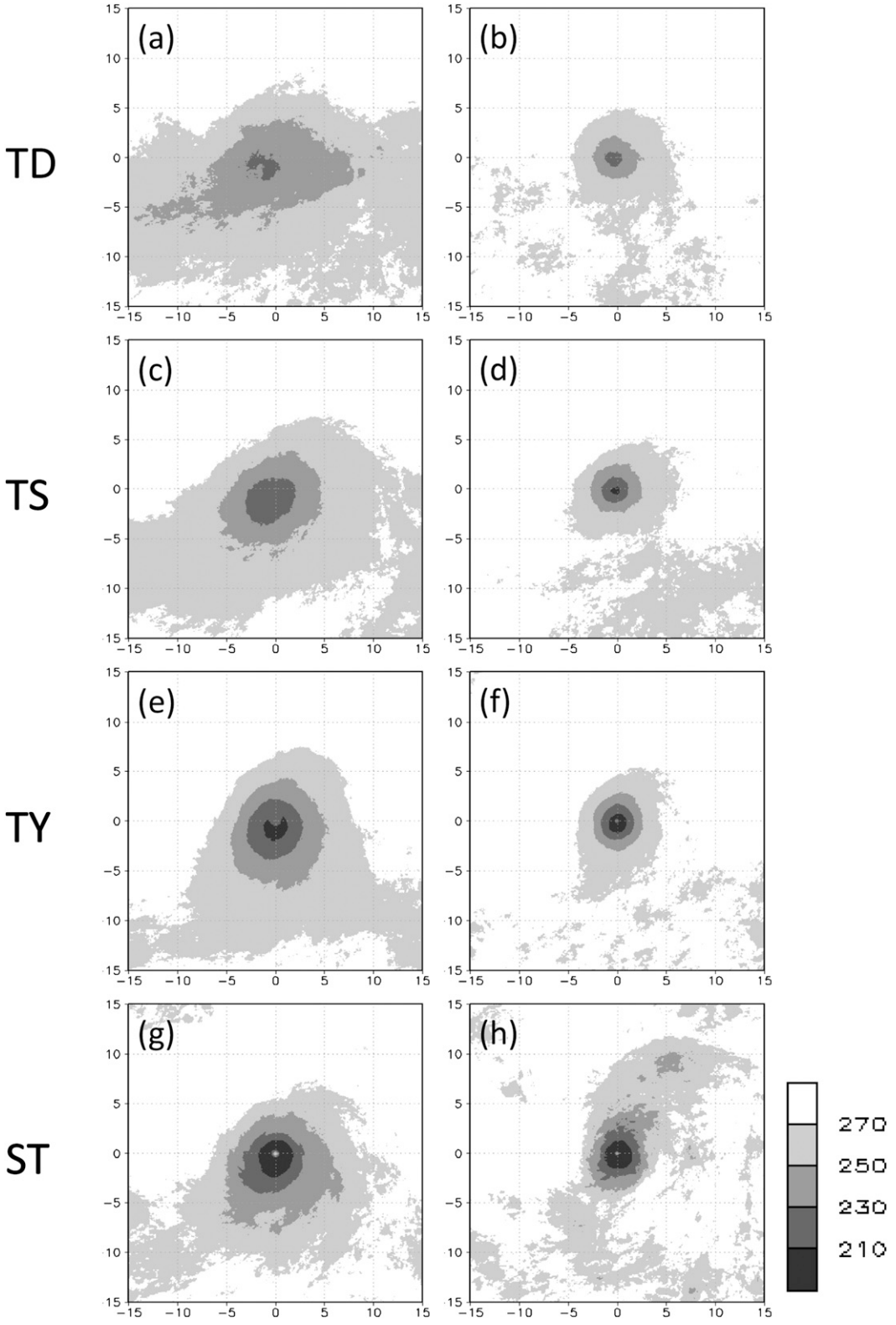

FIG. 7. Composite cloud-top temperature (K) relative to the TC center for different development phases (TD, TS, TY, and ST). (a),(c),(e),(g) Incompact TCs, and (b),(d),(f),(h) compact cases are shown. The domain of each panel is 30° latitude × 30° longitude.

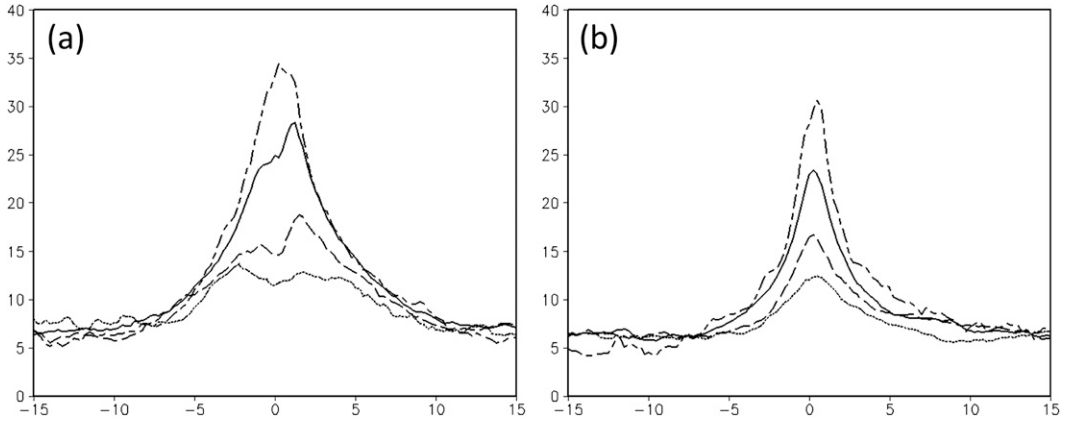

FIG. 8. Cross section through the TC center of the composite QuikSCAT 10-m wind speed (m s^{-1}) for (a) incompact TCs and (b) compact TCs at TD (dotted), TS (dashed), TY (solid), and ST (dot–dashed) stages.

a relatively broad area of strong wind during the tropical depression and tropical storm stages. There are multiple wind maxima in the profiles, which may be associated with convective systems embedded within the system or triggered by environmental flow. During intensification, the growth of the wind profile is mainly within 5° latitude × 5° longitude from the TC center. By contrast, compact TCs have an already well-defined wind structure at the tropical storm stage, and during intensification the strong wind concentrates within only about 2.5° latitude × 2.5° longitude from the center.

c. *Environmental conditions*

Composites of 850-hPa flow according to different intensities and the compactness of the cases are formed (Fig. 9). To measure variability within these composite wind fields, a steadiness value defined as

$$\text{Steadiness} = (\text{magnitude of composite wind vector}) / (\text{mean wind speed}) \times 100\% \quad (5)$$

is calculated for each composite as an indicator of its validity (Cheung and Elsberry 2002). The steadiness value has a high percentage if the wind structures in all composite members are about the same. The differences in the low-level circulations associated with the compact and incompact cases agree with those inferred from comparing their respective cloud-top temperature composites. During the tropical depression stage, stronger environmental westerlies and southwesterlies about 5°–10° latitude south of the TC center are found for the incompact cases, which are robust features in the composite because steadiness of over 90% is found in that region. These westerlies and southwesterlies lead to strong low-level convergence with the TC circulation that triggers the extensive areas of convection as depicted in satellite images. Consequently, low-level relative vorticity outside the core region of these cases can increase because of the convection, hence making them incompact in structure. This situation continues until tropical storm intensity is reached (and again robustness is indicated by a high steadiness value in composites) because the difference in wind field of incompact TCs relative to the compact TCs still shows positive value at about 5° latitude south of the center (Fig. 9c). When intensifying to typhoon and supertyphoon stages, both the compact and incompact TCs show the familiar wavenumber-1 structure with the maximum wind speed located at northeast of center. The differences in wind field at these two intensity stages are azimuthally symmetric and mainly account for the larger wind speed outside the core region of the incompact TCs compared with the compact TCs.

Therefore, one can infer from both the composite satellite images and wind flows that the environment in which TCs form plays an important role in determining if they develop initially into more compact TCs, while during further intensification these TCs can maintain their compact structures through internal dynamics. To understand the other possible synoptic factors that determine the compactness of TCs other than convection and low-level wind flow, the parameters based on the predictors in the Statistical Hurricane Intensity Prediction Scheme (SHIPS; DeMaria and Kaplan 1994a, 1999; DeMaria et al. 2005) and the Statistical Typhoon Intensity Prediction Scheme (STIPS; Fitzpatrick 1997; Knaff et al. 2005) are examined. These include average angular momentum and relative vorticity, and its horizontal advection, temperature, divergence, gradient of cloud-top temperature, zonal wind, and relative humidity at various levels and distances from the center. They are readily calculated using NCEP GFS analyses and satellite

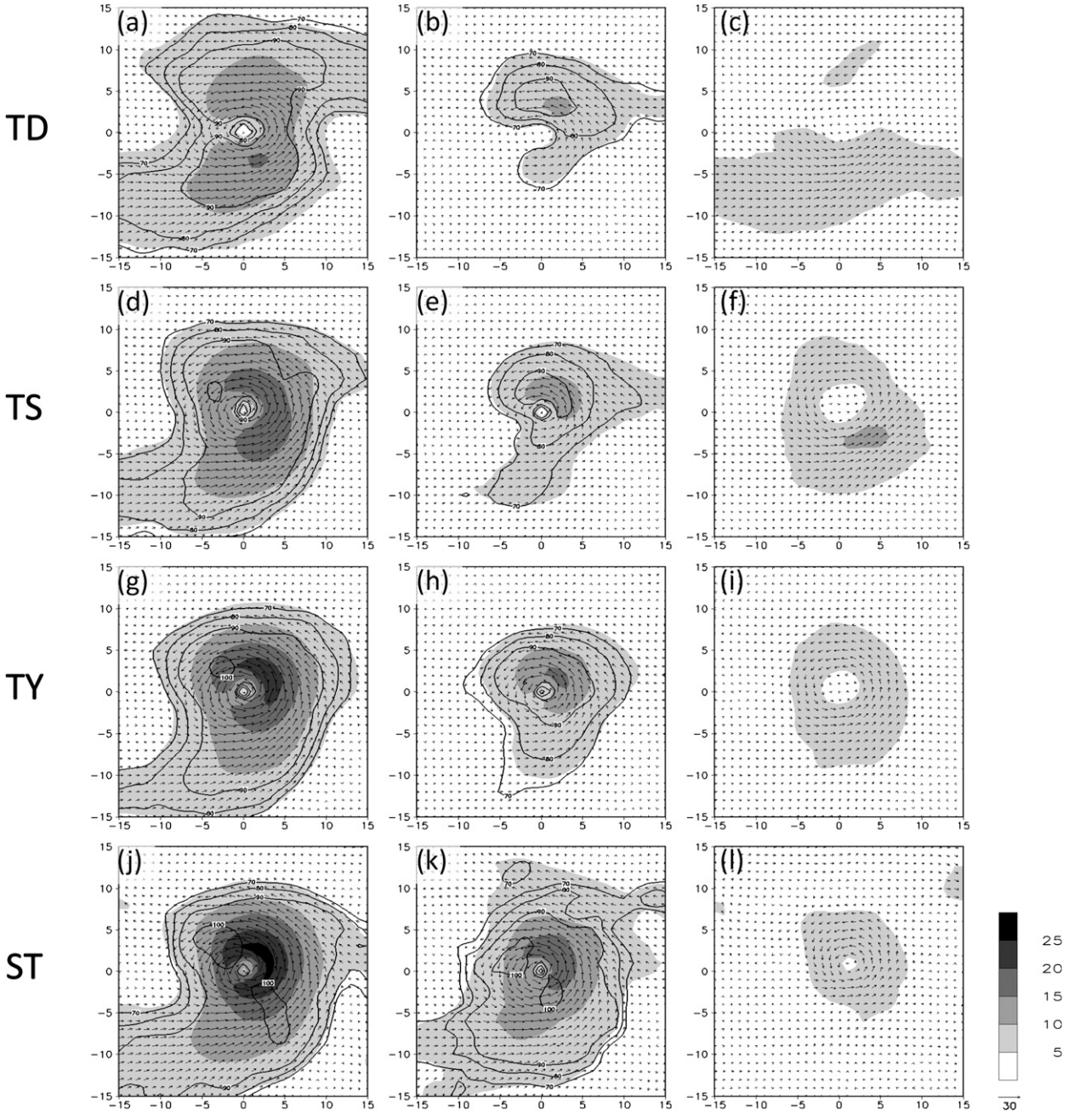

FIG. 9. Composite 850-hPa wind speed (shaded) and wind vector (arrows) at TD, TS, TY, and ST stages, respectively. Contours denote steadiness at the 70%, 80%, and 90% levels. (a),(d),(g),(j) Incompact TCs, (b),(e),(h),(k) compact TCs, and (c),(f),(i),(l) difference fields between the incompact and compact TCs are shown. The domain of each panel is 30° latitude × 30° longitude.

IR1 data. Before examining these parameters, it is emphasized that no attempt is made to separate the environmental forcing from the TC circulation. The composite analyses for some of the parameters within selected regions focus on mean environmental fields, and try to identify the essential features during development of the compact TCs.

Only a few parameters are useful for distinguishing compact versus incompact TCs. One example is the MUND parameter (following the study of Mundell 1990), which is the ratio of inner-core convection (0°–2° latitude × longitude with brightness temperature Tb < -75°C) to outer-core convection (2°–6° latitude × longitude with Tb < -65°C; see Fitzpatrick 1997). Mundell (1990)

TABLE 2. Environmental parameters computed for all, incompact, compact, and extremely compact TC cases. MUND is the ratio of inner- to outer-core convection; TD-Int/MPI is the ratio of average intensity to average maximum potential intensity at TD stage, and similarly for TS-Int/MPI, TY-Int/MPI, and ST-Int/MPI; 2DIVG300 is the average 200-hPa divergence (10^{-5} s^{-1}) within 300 km from the TC center, and similarly for 2DIVG400 and 2DIVG500; 8–7RH300 is the average 850–700-hPa relative humidity within 300 km from the TC center, and similarly for 8–7RH400 and 8–7RH500.

Parameter	All cases	Incompact cases	Compact cases	Extremely compact cases
MUND	10.17	3.68	22.37	33.74
TD-Int/MPI	18.5%	18.5%	18.6%	18.2%
TS-Int/MPI	33.2%	32.3%	33.9%	32.1%
TY-Int/MPI	62.1%	60.4%	62.1%	61.8%
ST-Int/MPI	92.6%	91.9%	97.5%	84.0%
2DIVG300	0.52	0.72	0.38	0.38
2DIVG400	0.47	0.67	0.30	0.29
2DIVG500	0.40	0.56	0.24	0.23
8–7RH300	81.2%	84.5%	78.0%	77.7%
8–7RH400	80.3%	83.8%	77.0%	76.8%
8–7RH500	79.1%	82.7%	75.9%	75.9%

developed a scheme that uses MUND to forecast rapid intensification within 12 h, and the parameter is used to describe the gradient of cloud-top temperature here. As expected, the average MUND value of compact TCs is nearly 2 times that of incompact cases (Table 2). For extremely compact cases (defined as $S \leq 0.5$, which is the 10th percentile of all S parameters), the MUND value is much higher.

Next, the ratio of TC intensity to maximum potential intensity (MPI) is examined (Emanuel 1988; Holland 1997). Because this intensity to the MPI ratio usually increases substantially during intensification of a TC, instead of considering this trend for individual cases, the ratio of the average intensity to the average MPI is calculated. This is done for all TC cases and subsets of them (the incompact, compact, and extremely compact cases; see Table 2). For TCs at tropical storm, typhoon, and supertyphoon intensity categories, the compact cases on average attain intensities that are closer to the MPI compared with the incompact cases. This slightly higher intensification efficiency associated with compact TCs is likely due to the fact that they have concentrated convection within the inner core. The spinning up of the wind speed near the center increases the intensity more effectively compared with the incompact cases. It is noted that the differences between the incompact and extremely compact cases for all intensity categories are very small, but because the extremely compact cases represent only the first 10% of all TCs according to the ranking by the S parameter, statistically robust conclusions are difficult to make because of the small sample size in this category.

Two other parameters that show larger deviations between incompact and compact (and extremely compact) TCs are the upper-level (200 hPa) divergence and lower-level (850–700 hPa) relative humidity (Table 2). The average values of the former within 300–500 km from the center for incompact TCs are about double those for compact ones, which is attributed to the more extended convection in incompact TCs that results in a larger area with strong upper-level divergence. For relative humidity, the average values within 300–500 km from the center for incompact TCs are about 7% higher than the compact and extremely compact cases. This is consistent with the recent studies of Wang (2008) and Hill and Lackmann (2009), which suggest that environmental relative humidity is a crucial factor controlling TC size by modulating precipitation and thus latent heat release outside the core region. The potential vorticity distribution is then more extended, and this is favorable for lateral wind field expansion in the outer portion. However, convection in compact TCs is confined to a small region near the center, and to what extent relative humidity is controlling their development needs further investigation. Other parameters, such as relative vorticity, vertical wind shear, and relative eddy angular momentum flux convergence are not significantly different in compact versus incompact TCs.

Maclay et al. (2008) suggested two primary types of TC growth processes as indicated by a positive KE deviation. One of them consists of internally dominated processes, such as secondary eyewall formation and eyewall replacement. The other pertains to external forcing from the synoptic environment, such as vertical shear and temperature advection in the near-storm environment. Based on analysis of environmental parameters, this study shows that certain low-level synoptic patterns are more favorable for the formation of incompact TCs. On the other hand, dry environments seem to be more favorable for the development of compact TCs. One of the difficulties in comparing these coarse-resolution parameters based on the analysis of large-scale datasets is that they do not allow for detailed examination of the processes in the TC core region during intensification, which is believed to largely determine the compactness of the system. Therefore, numerical simulations of typical compact and incompact typhoons will be carried out for diagnosis and reported in a separate study.

5. Summary and discussion

This study focuses on TCs in the WNP with compact structure, which differs substantially from the general vortex structure, and especially from those with extended rainband structures. Compact TCs often have strong

convection concentrated around the eye with an area free of convection surrounding the convective ring. Similar to the AHs that have large radii of maximum wind, these TCs are seldom accompanied by active rainbands, but at the same time they possess relatively small eye radii. The ratios of intensity to MPI are larger than an average TC for both AHs and compact TCs.

The usual measures of TC structure, namely intensity, strength, and size, are quite inadequate for describing the evolution of compact TCs (Powell and Reinhold 2007; Maclay et al. 2008). Therefore, a new structure parameter S is defined in this study. In addition to having similar characteristics as the b parameter in a Rankine vortex [Eq. (3)], the S parameter also includes specific information about the relationship between TC intensity, Vt_{max}, and RMW. It is generally known that TC intensity is more determined by inner-core dynamics and TC size is more related to outer-core evolution, leading to a low correlation between observed intensity and size (Lee et al. 2010, and references therein). The S parameter can serve as a complementary measure that indicates the relative evolution of the inner- and outer-core regions.

Examination of the compactness of 171 TCs in the years 2000–07 during their various developmental stages reveals that the percentage of compact TCs is much larger than that of incompact TCs during the early intensification stage; that is, a compact structure is quite conducive to intensification. Compact TCs are associated with intensification rates of about 10 m s^{-1} in 24 h, while incompact TCs are more associated with decay rates of about 5–15 m s^{-1} in 24 h. This is consistent with the recent findings of Knaff et al. (2010), which show that weaker TCs tend to become small with slower translation speeds at lower latitudes, and their 12-h intensification rates are larger than those for the more intense TCs. When compact TCs intensify to typhoons or supertyphoons, their average intensities are closer to the average MPIs compared to incompact cases, implying higher efficiency of intensification in TCs with compact structures. When examining different moving directions, the results show that more incompact cases are northward-moving TCs, while mostly compact cases are westward-moving TCs.

Compact and incompact TCs exhibit different convection patterns, based on analysis of composite infrared cloud-top temperature. One distinguishable feature is that persistent convective activities are identified in the incompact cases at about 5° latitude or more southwest of the TC center, and collocate with environmental southwesterlies. In contrast, the composites of infrared cloud-top temperature for compact TCs show a fairly axisymmetric structure of deep convection in the inner-core region. In other words, the role of low-level external environmental forcing is more important in the development of incompact TCs, while mainly internal dynamics are crucial to the development of compact TCs. However, in addition to the low-level synoptic pattern there seems to be few large-scale environmental parameters that can be used to distinguish compact and incompact TCs. One such parameter is low-level relative humidity near the TC center that is known to control outer-core convection and increase wind speed (and, hence, TC size), but its exact role in determining compactness has to be investigated further.

The increase in strength or size requires a substantial import of angular momentum (Holland 1983). For example, as seen in the modeling experiments of Challa and Pfeffer (1980), angular momentum flux convergence markedly accelerates the development of TCs. Because there are almost no well-defined rainband features in compact TCs, a minimal increase of wind speed occurs in the outer-core region. It can be hypothesized that the mechanisms that leads to the development of compact TCs are closely related to strong inner-core convective heating or the strong divergence provided from the upper-level outflow region. However, the average values of upper-level divergence within 300–500 km from the TC center for compact TCs are actually lower than those for incompact TCs, which should be attributed to the more extended outflow structures associated with the latter cases. More refined techniques to compare the contribution from near-eyewall convection in the two TC categories are necessary. Compared with the analyses of KE in Maclay et al. (2008), this study provides a different method to detect the inner-core wind structure of TCs. Nevertheless, this study leads to a similar conclusion that internal dynamics play an important role in TC structural change, especially for compact TCs.

With forecasting issues in mind, the objective identification of compact TCs in an operational setting can help forecasters to better predict future intensity changes for these TCs, and possibly reduce overall intensity forecast errors. Better mitigation measures can also be prepared for localized heavy rainfall and strong gust winds associated with compact TCs when they make landfall. For this purpose, similar models to the annular hurricane detection algorithm (Knaff et al. 2003, 2008) can be developed based on the results of this study.

Acknowledgments. Comments and suggestions from Dr. John Knaff and the anonymous reviewer improved the manuscript substantially, and are much appreciated. This research is supported by the National Science Council of the Republic of China (Taiwan) under Grants NSC97-2625-M-002-002 and NSC 98-2625-M-002-002.

The participation of the second author (KKWC) in this study is supported by the Macquarie University Research Development Grant 9201000735.

REFERENCES

Bender, M. A., and I. Ginis, 2000: Real-case simulations of hurricane–ocean interaction using a high-resolution coupled model: Effects on hurricane intensity. *Mon. Wea. Rev.,* **128,** 917–946.

Black, M. L., and H. E. Willoughby, 1992: The concentric eyewall cycle of Hurricane Gilbert. *Mon. Wea. Rev.,* **120,** 947–957.

Boukabara, S.-A., R. N. Hoffman, C. Grassotti, and S. M. Leidner, 2002: Physically based modeling of QSCAT SeaWinds passive microwave measurements for rain detection. *J. Geophys. Res.,* **107,** 4786, doi:10.1029/2001JD001243.

Bourassa, M. A., D. M. Legler, J. J. O'Brien, and S. R. Smith, 2003: SeaWinds validation with research vessels. *J. Geophys. Res.,* **108,** 3019–3034.

Brand, S., 1972: Very large and very small typhoons of the western North Pacific Ocean. *J. Meteor. Soc. Japan,* **50,** 332–341.

Brennan, M. J., C. C. Hennon, and R. D. Knabb, 2009: The operational use of QuikSCAT ocean surface vector winds at the National Hurricane Center. *Wea. Forecasting,* **24,** 621–645.

Carr, L. E., III, and R. L. Elsberry, 1997: Models of tropical cyclone wind distribution and beta-effect propagation for application to tropical cyclone track forecasting. *Mon. Wea. Rev.,* **125,** 3190–3209.

Challa, M., and R. L. Pfeffer, 1980: Effects of eddy fluxes of angular momentum on model hurricane development. *J. Atmos. Sci.,* **37,** 1603–1618.

Chan, J. C.-L., and R. T. Williams, 1987: Analytical and numerical studies of the beta-effect in tropical cyclone motion. Part I: Zero mean flow. *J. Atmos. Sci.,* **44,** 1257–1265.

Cheung, K. K. W., and R. L. Elsberry, 2002: Tropical cyclone formations over the western North Pacific in the Navy Operational Global Atmospheric Prediction System Forecasts. *Wea. Forecasting,* **17,** 800–820.

Cocks, S. B., and W. M. Gray, 2002: Variability of the outer wind profiles of western North Pacific typhoons: Classifications and techniques for analysis and forecasting. *Mon. Wea. Rev.,* **130,** 1989–2005.

Croxford, M., and G. M. Barnes, 2002: Inner core strength of Atlantic tropical cyclones. *Mon. Wea. Rev.,* **130,** 127–139.

Cubukcu, N., R. L. Pfeffer, and D. E. Dietrich, 2000: Simulation of the effects of bathymetry and land–sea contrasts on hurricane development using a coupled ocean–atmosphere model. *J. Atmos. Sci.,* **57,** 481–492.

DeMaria, M., 1996: The effect of vertical shear on tropical cyclone intensity change. *J. Atmos. Sci.,* **53,** 2076–2087.

——, and J. Kaplan, 1994a: A Statistical Hurricane Intensity Prediction Scheme (SHIPS) for the Atlantic basin. *Wea. Forecasting,* **9,** 209–220.

——, and ——, 1994b: Sea surface temperature and the maximum intensity of Atlantic tropical cyclones. *J. Climate,* **7,** 1324–1334.

——, and ——, 1999: An updated Statistical Hurricane Intensity Prediction Scheme (SHIPS) for the Atlantic and eastern North Pacific basins. *Wea. Forecasting,* **14,** 326–337.

——, M. Mainelli, L. K. Shay, J. A. Knaff, and J. Kaplan, 2005: Further improvements to the Statistical Hurricane Intensity Prediction Scheme (SHIPS). *Wea. Forecasting,* **20,** 531–543.

Ebuchi, N., H. C. Graber, and M. J. Caruso, 2002: Evaluation of wind vectors observed by QuikSCAT/SeaWinds using ocean buoy data. *J. Atmos. Oceanic Technol.,* **19,** 2049–2062.

Emanuel, K. A., 1988: The maximum intensity of tropical cyclones. *J. Atmos. Sci.,* **45,** 1143–1155.

——, C. DesAutels, C. Holloway, and R. Korty, 2004: Environmental control of tropical cyclone intensity. *J. Atmos. Sci.,* **61,** 843–858.

Fitzpatrick, P. J., 1997: Understanding and forecasting tropical cyclone intensity change with the Typhoon Intensity Prediction Scheme (TIPS). *Wea. Forecasting,* **12,** 826–845.

Frank, W. M., and W. M. Gray, 1980: Radius and frequency of 15 m s^{-1} (30 kt) winds around tropical cyclones. *J. Appl. Meteor.,* **19,** 219–223.

——, and E. A. Ritchie, 2001: Effects of vertical wind shear on the intensity and structure of numerically simulated hurricanes. *Mon. Wea. Rev.,* **129,** 2249–2269.

Guard, C. P., L. E. Carr, F. H. Wells, R. A. Jeffries, N. D. Gural, and D. K. Edson, 1992: Joint Typhoon Warning Center and the challenges of multibasin tropical cyclone forecasting. *Wea. Forecasting,* **7,** 328–352.

Guinn, T. A., and W. H. Schubert, 1993: Hurricane spiral bands. *J. Atmos. Sci.,* **50,** 3380–3404.

Hill, K. A., and G. M. Lackmann, 2009: Influence of environmental humidity on tropical cyclone size. *Mon. Wea. Rev.,* **137,** 3294–3315.

Holland, G. J., 1983: Angular momentum transports in tropical cyclones. *Quart. J. Roy. Meteor. Soc.,* **109,** 187–210.

——, 1997: The maximum potential intensity of tropical cyclones. *J. Atmos. Sci.,* **54,** 2519–2541.

——, and R. T. Merrill, 1984: On the dynamics of tropical cyclone structural changes. *Quart. J. Roy. Meteor. Soc.,* **110,** 723–745.

Knaff, J. A., and R. M. Zehr, 2007: Reexamination of tropical cyclone pressure wind relationships. *Wea. Forecasting,* **22,** 71–88.

——, J. P. Kossin, and M. DeMaria, 2003: Annular hurricanes. *Wea. Forecasting,* **18,** 204–223.

——, S. A. Seseske, M. DeMaria, and J. L. Demuth, 2004: On the influences of vertical wind shear on symmetric tropical cyclone structure derived from AMSU. *Mon. Wea. Rev.,* **132,** 2503–2510.

——, C. R. Sampson, and M. DeMaria, 2005: An operational statistical typhoon intensity prediction scheme for the western North Pacific. *Wea. Forecasting,* **20,** 688–699.

——, T. A. Cram, A. B. Schumacher, J. P. Kossin, and M. DeMaria, 2008: Objective identification of annular hurricanes. *Wea. Forecasting,* **23,** 17–28.

——, D. P. Brown, J. Courtney, G. M. Gallina, and J. L. Beven II, 2010: An evaluation of Dvorak technique-based tropical cyclone intensity estimates. *Wea. Forecasting,* **25,** 1362–1379.

Kossin, J. P., and M. D. Eastin, 2001: Two distinct regimes in the kinematic and thermodynamic structure of the hurricane eye and eyewall. *J. Atmos. Sci.,* **58,** 1079–1090.

——, J. A. Knaff, H. I. Berger, D. C. Herndon, T. A. Cram, C. S. Velden, R. J. Murnane, and J. D. Hawkins, 2007: Estimating hurricane wind structure in the absence of aircraft reconnaissance. *Wea. Forecasting,* **22,** 89–101.

Krayer, W. R., and R. D. Marshall, 1992: Gust factors applied to hurricane winds. *Bull. Amer. Meteor. Soc.,* **73,** 613–617.

Kuo, H.-C., C.-P. Chang, Y.-T. Yang, and H.-J. Jiang, 2009: Western North Pacific typhoons with concentric eyewalls. *Mon. Wea. Rev.,* **137,** 3758–3770.

Lee, C.-S., K. K. W. Cheung, W.-T. Fang, and R. L. Elsberry, 2010: Initial maintenance of tropical cyclone size in the western North Pacific. *Mon. Wea. Rev.,* **138,** 3207–3223.

Lin, I.-I., C.-C. Wu, K. Emanuel, I.-H. Lee, C.-R. Wu, and I.-F. Pun, 2005: The interaction of Super Typhoon Maemi (2003) with a warm ocean eddy. *Mon. Wea. Rev.,* **133,** 2635–2649.

——, ——, I.-F. Pun, and D.-S. Ko, 2008: Upper-ocean thermal structure and the western North Pacific category 5 typhoons. Part I: Ocean features and the category 5 typhoons' intensification. *Mon. Wea. Rev.,* **136,** 3288–3306.

Liu, K. S., and J. C. L. Chan, 1999: Size of tropical cyclones as inferred from *ERS-1* and *ERS-2* data. *Mon. Wea. Rev.,* **127,** 2992–3001.

Maclay, K. S., M. DeMaria, and T. H. V. Harr, 2008: Tropical cyclone inner-core kinetic energy evolution. *Mon. Wea. Rev.,* **136,** 4882–4898.

Mainelli, M., M. DeMaria, L. K. Shay, and G. Goni, 2008: Application of oceanic heat content estimation to operational forecasting of recent Atlantic category 5 hurricanes. *Wea. Forecasting,* **23,** 3–16.

Merrill, R. T., 1984: A comparison of large and small tropical cyclones. *Mon. Wea. Rev.,* **112,** 1408–1418.

Mueller, K. J., M. DeMaria, J. Knaff, J. P. Kossin, and T. H. V. Harr, 2006: Objective estimation of tropical cyclone wind structure from infrared satellite data. *Wea. Forecasting,* **21,** 990–1005.

Mundell, D. B., 1990: Prediction of tropical cyclone rapid intensification events. M.S. thesis, Dept. of Atmospheric Science, Colorado State University, 186 pp. [Available from Dept. of Atmospheric Science, Colorado State University, Fort Collins, CO 80523.]

Pickett, M. H., W. Tang, L. K. Rosenfeld, and C. H. Wash, 2003: QuikSCAT satellite comparison with nearshore buoy wind data off the U.S. West Coast. *J. Atmos. Oceanic Technol.,* **20,** 1869–1879.

Powell, M., and T. Reinhold, 2007: Tropical cyclone destructive potential by integrated kinetic energy. *Bull. Amer. Meteor. Soc.,* **88,** 513–526.

Sampson, C. R., R. A. Jeffries, C. J. Neumann, and J.-H. Chu, 1995: Tropical cyclone intensity. Tropical Cyclone Forecasters' Reference Guide, NRL Rep. NRL/PU/7541–95-0012, 34 pp.

Schade, L. R., 2000: Tropical cyclone intensity and sea surface temperature. *J. Atmos. Sci.,* **57,** 3122–3130.

Schubert, W. H., M. T. Montgomery, R. K. Taft, T. A. Guinn, S. R. Fulton, J. P. Kossin, and J. P. Edwards, 1999: Polygonal eyewalls, asymmetric eye contraction, and potential vorticity mixing in hurricanes. *J. Atmos. Sci.,* **56,** 1197–1223.

Sharma, N., and E. D'Sa, 2008: Assessment and analysis of QuikSCAT vector wind products for the Gulf of Mexico: A long-term and hurricane analysis. *Sensors,* **8,** 1927–1949.

Wang, Y., 2008: What controls tropical cyclone size and intensity. *IPRC Climate,* Vol. 8, No. 2, International Pacific Research Center, 3–5.

Weatherford, C., and W. M. Gray, 1988: Typhoon structure as revealed by aircraft reconnaissance. Part II: Structural variability. *Mon. Wea. Rev.,* **116,** 1044–1056.

Weissman, D. E., M. A. Bourassa, and J. Tongue, 2002: Effects of rain rate and wind magnitude on SeaWinds scatterometer wind speed errors. *J. Atmos. Oceanic Technol.,* **19,** 738–746.

Wu, C.-C., C.-Y. Lee, and I.-I. Lin, 2007: The effect of the ocean eddy on tropical cyclone intensity. *J. Atmos. Sci.,* **64,** 3562–3578.

Weather and Forecasting

Title Details | Table of Contents

Basic Description

Title	Weather and Forecasting
ISSN	0882-8156
Publisher	American Meteorological Society
Country	United States
Status	Active
Start Year	1986
Frequency	Bi-monthly
Language of Text	Text in: English
Refereed	Yes
Abstracted / Indexed	Yes
Serial Type	Journal
Content Type	Academic / Scholarly
Format	Print
Website	http://www.ametsoc.org/pubs/journals/waf/index.html
Email	waf@atmos.umd.edu
Description	Features operational forecasting techniques, applications of new analysis methods, forecasting verification studies, and meso-scale and synoptic-scale case studies that have direct applicability to forecasting.